MAXIMUM LIKELIHOOD TEXTURE TRACKING IN HIGHLY HETEROGENEOUS POLSAR CLUTTER

Olivier Harant[1,2], *Lionel Bombrun*[1], *Gabriel Vasile*[1], *Laurent Ferro-Famil*[2], *Michel Gay*[1]

[1] Grenoble-Image-sPeech-Signal-Automatics Lab
GIPSA-lab DIS/SIGMAPHY, CNRS
Grenoble INP, 961 rue de la Houille Blanche, BP 46 38402 Grenoble, France

[2] Institute of Electronics and Telecommunications Rennes
IETR SAPHIR, CNRS
Université de Rennes 1, Bat. 11D, 263 avenue du Général Leclerc 35042 Rennes, France

1. INTRODUCTION

The new generation of high resolution SAR sensors are able to produce high quality images of the Earth's surface. As the number of scatterers per resolution cell decreases, heterogeneous clutter model should be used to extract information. In this context, Spherically Invariant Random Vector (SIRV) have been introduced. The Polarimetric SAR (PolSAR) target vector $\mathbf{k}$ can be rewritten as the product between the square root of a positive random variable τ (representing the texture) and an independent complex Gaussian vector $\mathbf{z}$ with zero mean and covariance matrix $[M] = E\{\mathbf{z}\mathbf{z}^H\}$ (representing the speckle): $\mathbf{k} = \sqrt{\tau}\,\mathbf{z}$.

This paper introduces a new shift estimator based on the Fisher PDF for texture modeling. The proposed approach generalizes the Gamma PDF shift estimator introduced by Erten *et al.* in [1]. The general methodology employed for Maximum Likelihood (ML) texture tracking is exposed in section 2. Both models with uncorrelated and correlated texture between images are investigated. Next, some improvements of the conventional ML texture tracking algorithm are exposed in section 3. Finally, displacement results on synthetic and real images are presented in section 4.

2. MAXIMUM LIKELIHOOD TEXTURE TRACKING

Let $\mathbf{k}_x = [\mathbf{k}_{x_1}, \ldots, \mathbf{k}_{x_k}]$ and $\mathbf{k}_y^i = \left[\mathbf{k}_{y_1}^i, \ldots, \mathbf{k}_{y_k}^i\right]$ be two blocks of the PolSAR data-set containing k pixels. Subscripts x and y are referred respectively to the master and slave images. The texture blocks $\tau_x = [\tau_{x_1}, \ldots, \tau_{x_k}]$ and $\tau_y^i = \left[\tau_{y_1}^i, \ldots, \tau_{y_k}^i\right]$ are then estimated from the PolSAR data-set $\mathbf{k}_x$ and $\mathbf{k}_y^i$ according to the SIRV estimation scheme [2]. Those two texture blocks are shifted by a displacement called i. The ML texture tracking algorithm estimates the shift vector $\overrightarrow{v}_{\mathrm{ML}}$ which maximizes for each block i the Conditional Density Function (CDF) [1]. It yields:

$$\overrightarrow{v}_{\mathrm{ML}} = \underset{i}{\mathrm{Argmax}}\ p\left(\tau_x | \tau_y^i, \overrightarrow{v}_i\right) = \underset{i}{\mathrm{Argmax}}\ \prod_{j=1}^{k} \frac{1}{\tau_{y_j}^i}\, p_\alpha\left(\frac{\tau_{x_j}}{\tau_{y_j}^i}\right). \tag{1}$$

This work was supported by the French ANR program EFIDIR.

where $p_\alpha(\cdot)$ is the texture ratio PDF ($\alpha = \tau_x/\tau_y^i$).
In this paper, the Fisher PDF is introduced to model the texture parameter τ. Its PDF is given by:

$$p_\tau(\tau) = \mathcal{F}[m, \mathcal{L}, \mathcal{M}] = \frac{\Gamma(\mathcal{L}+\mathcal{M})}{\Gamma(\mathcal{L})\Gamma(\mathcal{M})} \frac{\mathcal{L}}{\mathcal{M}m} \frac{\left(\frac{\mathcal{L}\tau}{\mathcal{M}m}\right)^{\mathcal{L}-1}}{\left(1+\frac{\mathcal{L}\tau}{\mathcal{M}m}\right)^{\mathcal{L}+\mathcal{M}}} \tag{2}$$

where m is a scale parameter, $\mathcal{L}$ and $\mathcal{M}$ are two shape parameters. The Fisher PDF has been successfully validated to model the texture parameter of highly heterogeneous clutters [3]. Next, the texture ratio PDF p_α should be derived for both correlated and uncorrelated texture between images.

2.1. Texture model with uncorrelated texture between images

For a Fisher distributed texture, authors have established the texture ratio PDF for uncorrelated texture between images. Its expression is given by:

$$p_\alpha(\alpha) = \frac{B(2\mathcal{L}, 2\mathcal{M})}{[B(\mathcal{L}, \mathcal{M})]^2} \frac{1}{\alpha^{\mathcal{M}+1}} \times {}_2F_1\left(\mathcal{L}+\mathcal{M}, 2\mathcal{M}; 2(\mathcal{L}+\mathcal{M}); \frac{\alpha-1}{\alpha}\right) \tag{3}$$

where ${}_2F_1(\cdot, \cdot; \cdot; \cdot)$ and $B(\cdot, \cdot)$ are respectively the Gauss hypergeometric function and the Euler Beta function. Note that for uncorrelated texture between images, the scale parameter m simplifies when the texture ratio PDF is studied.

By combining (1) and (3), and following the same procedure as [1], the similarity measure is obtained:

$$\mathrm{ML}(\overrightarrow{v}_i) = k \ln\left(\frac{B(2\mathcal{L}, 2\mathcal{M})}{[B(\mathcal{L}, \mathcal{M})]^2}\right) - (\mathcal{M}+1)\sum_{j=1}^{k} \ln \tau_{x_j} + \mathcal{M}\sum_{j=1}^{k} \ln \tau_{y_j}^i + \sum_{j=1}^{k} {}_2F_1\left(\mathcal{L}+\mathcal{M}, 2\mathcal{M}; 2(\mathcal{L}+\mathcal{M}); 1 - \frac{\tau_{y_j}^i}{\tau_{x_j}}\right). \tag{4}$$

2.2. Texture model with correlated texture between images

The texture ratio PDF for correlated texture between images has been derived from the bivariate Fisher distribution [4]. Its expression is given by:

$$p_\alpha(\alpha) = \frac{R_1^{\mathcal{L}_1} R_2^{\mathcal{L}_2} B(\mathcal{L}_1+\mathcal{L}_2, \mathcal{M}_2)}{B(\mathcal{L}_1, \mathcal{M}_1) B(\mathcal{L}_2, \mathcal{L}_1+\mathcal{M}_2)} \times \frac{\alpha^{\mathcal{L}_1-1}}{(R_1\alpha + R_2)^{\mathcal{L}_1+\mathcal{L}_2}} \times {}_2F_1(a, b; c; z) \tag{5}$$

where $a = \mathcal{L}_1 + \mathcal{L}_2$, $b = \mathcal{M}_2 - \mathcal{M}_1$, $c = \mathcal{L}_1 + \mathcal{M}_2$, $z = \frac{1}{1+\frac{R_2}{R_1}\frac{1}{\alpha}}$, $R_1 = \frac{\mathcal{L}_1}{\mathcal{M}_1 m_1}$ and $R_2 = \frac{\mathcal{L}_2}{\mathcal{M}_2 m_2}$.
Similarly, combining (1) and (5) yields to:

$$\begin{aligned}\mathrm{ML}(\overrightarrow{v}_i) &= k\mathcal{L}_1 \ln R_1 + k\mathcal{L}_2 \ln R_2 + k \ln\left(\frac{B(\mathcal{L}_1+\mathcal{L}_2, \mathcal{M}_2)}{B(\mathcal{L}_1, \mathcal{M}_1) B(\mathcal{L}_2, \mathcal{L}_1+\mathcal{M}_2)}\right) \\ &+ \sum_{j=1}^{k} \mathcal{L}_1 \ln \frac{\tau_{x_j}}{\tau_{y_j}^i} - \ln \tau_{x_j} - (\mathcal{L}_1+\mathcal{L}_2) \ln\left(R_1 \frac{\tau_{x_j}}{\tau_{y_j}^i} + R_2\right) + {}_2F_1(a, b; c; z_j).\end{aligned} \tag{6}$$

3. ADVANCED SIGNAL PROCESSING ISSUE FOR DISPLACEMENT ESTIMATION

Classical ML texture tracking uses rectangular sliding window. As the derived criteria are issued from statistical modeling, authors proposed to adapt the sliding window instead of the conventional rectangular one. Moreover, as motion estimation is often used in a geophysical monitoring context (glacier, volcano, ...), it could be judicious to add a physical flow model constraint. This regularisation step is introduced through the Bayes's rule.

3.1. Adaptive Offset Estimation

As the ML texture tracking algorithm studies the statistic of the population, the considered area should be homogeneous in term of stochastic process. The proposed approach consists in partitioning the data-set. A ML hierarchical segmentation algorithm is adapted to the multivariate KummerU distribution (texture is Fisher distributed) [3]. Fig. 1(b) shows an example of segmentation of a crevasses field on the Argentière glacier in the Mont-Blanc massif. Then, for each segment, the ML texture tracking is computed considering that the motion is uniform on each segment.

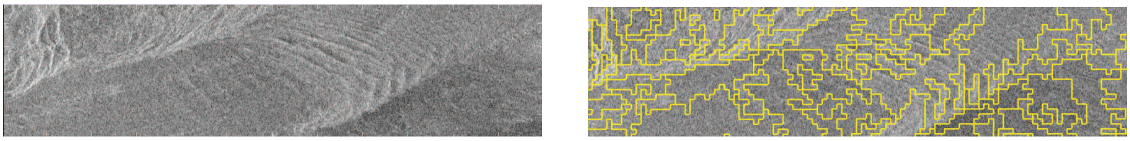

(a) (b)

Fig. 1. Logarithm of the texture parameter τ estimated using SIRV model (a). Hierarchical segmentation (b). TSX data 2009-01-06. Argentière glacier.

3.2. Bayes Inference for Flow Model Constraint

In the context of geophysical objects motion, *a priori* flow model can be combined with the similarity measure to derive the displacement field. According to the Bayes's rule, the problem formulation becomes:

$$p\left(\tau_y^i, \overrightarrow{v}_i | \tau_x^i\right) = \frac{p\left(\tau_x^i | \tau_y^i, \overrightarrow{v}_i\right) p\left(\tau_y^i | \overrightarrow{v}_i\right) p\left(\overrightarrow{v}_i\right)}{p\left(\tau_x^i\right)} \tag{7}$$

Let v_i^d and v_i^{az} be respectively the two components of the displacement vector $\overrightarrow{v}_i$ along the distance and azimuth direction. In (7), the prior term $p\left(\overrightarrow{v}_i\right)$ can be rewritten as:

$$p\left(\overrightarrow{v}_i\right) = p\left(v_i^d\right) p\left(v_i^{az}\right) = \rho_i \, p_\rho\left(\rho_i\right) \; p_\theta\left(\theta_i\right) \tag{8}$$

where ρ_i and θ_i are the polar coordinates of the displacement vector $\overrightarrow{v}_i$. They are linked with the distance and azimuth component by $\rho_i = \sqrt{v_i^{d2} + v_i^{az2}}$ and $\theta_i = \text{atan}(v_i^{az}/v_i^d)$.

For example, when only one Line Of Sight (LOS) displacement projection is avalable, additionnal assumption need to be taken into account for deriving the 3D displacement field. In the context of glacier monitoring, these assumptions can be a flow parallel to the glacier surface in the direction of the maximum downhill slope. Such information can be included in the proposed prior model from eq. (7). The orientation angle θ_i is assumed to be normally distributed and has circular values between $-\pi$ and $+\pi$. The orientation angle follows the Von Mises distribution (also known as the circular normal distribution) which is the circular analogue of the normal distribution [5]. Concerning the absolute value of the displacement ρ_i, no constraint is imposed. ρ_i is therefore assumed to be uniformly distributed in the search neighbourhood.

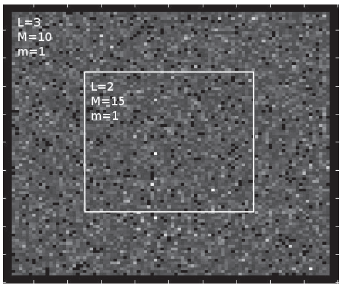

(a) Simulated texture sampled from two Fisher PDF. There is no motion between master and slave images

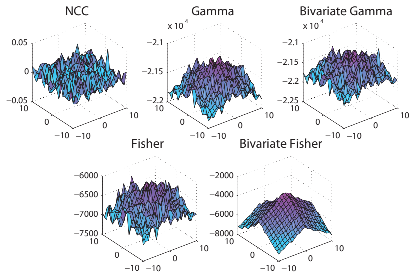

(b) Detection surfaces for the multiplicative noised dataset: NCC, uncorrelated and correlated Gamma ML, uncorrelated and correlated Fisher ML.

Fig. 2. Displacement results on the synthetic dataset

4. PRELIMINARY RESULTS

To evaluate the potential of the proposed ML texture tracking algorithm, a synthetic dataset has been simulated. This dataset is composed by two areas (Fig. 2(a)). The border and the center are respectively generated from two Fisher PDFs. The algorithm is executed with a sliding rectangular window which matches exactly the center area.

Detection surfaces with the normalized cross-correlation coefficient (NCC), the ML texture tracking algorithm with Gamma and Fisher PDFs for both uncorrelated and correlated texture between images are shown in Fig. 2(b).

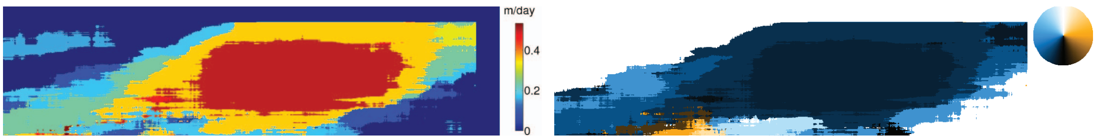

Fig. 3. Displacement estimation over a crevasse area on the Argentière glacier using a 64×256 pixels sliding window. Displacement field in LOS (*left*) and orientation map (*right*). Dual-pol TSX data, 2009-01-06 / 2009-02-08.

An application of the ML texture tracking algorithm on the Argentière glacier (Mont Blanc massif, France) is exposed in Fig. 3. Further results and discussions on shift estimation will be added in the final version of the paper. Displacement results with RADARSAT-2 quad-pol data will also analyzed on the whole glacier surface.

5. REFERENCES

[1] E. Erten, A. Reigber, O. Hellwich, and P. Prats, "Glacier Velocity Monitoring by Maximum Likelihood Texture Tracking," *IEEE Transactions on Geoscience and Remote Sensing*, vol. 47, no. 2, pp. 394–405, 2009.

[2] F. Pascal, P. Forster, J. P. Ovarlez, and P. Larzabal, "Performance Analysis of Covariance Matrix Estimates in Impulsive Noise," *IEEE Transactions on Signal Processing*, vol. 56, no. 6, pp. 2206–2216, 2008.

[3] L. Bombrun, J.-M. Beaulieu, G. Vasile, J.-P. Ovarlez, F. Pascal, and M. Gay, "Hierarchical Segmentation of Polarimetric SAR Images using Heterogeneous Clutter Models," in *IEEE International Geoscience and Remote Sensing Symposium, IGARSS '09, South Africa*, 2009.

[4] A.H. El-Bassiouny and M. Jones, "A Bivariate F Distribution with Marginals on Arbitrary Numerator and Denominator Degrees of Freedom, and Related Bivariate Beta and t Distributions," *Statistical Methods and Applications*, 2008.

[5] M. Abramowitz and I.A. Stegun, *Handbook of Mathematical Functions With Formulas, Graphs, and Mathematical Tables*, 1964.